Molecular Dynamics Simulations of Poly(3-hexylthiophenes) in Dilute Solutions

Stephanie M. Hoffmann

A thesis

submitted in partial fulfillment of the

requirements for the degree of

Master of Science

University of Washington

2014

Committee:

Jim Pfaendtner

Xiaosong Li

Program Authorized to Offer Degree:

Chemical Engineering

University of Washington

Abstract

Molecular Dynamics Simulations of Poly(3-hexylthiophenes) in Dilute Solutions

Stephanie M. Hoffmann

Chair of the Supervisory Committee:
Professor Jim Pfaendtner, Ph.D.
Chemical Engineering

Conjugated polymers hold exciting potential in the field of organic electronics. As compared with traditional devices, polymer-based electronic devices are cheaper, lighter, and more easily processed. Molecular dynamics (MD) simulation is a useful tool for the study of these polymers because it allows us to probe structural properties at a length scale unobtainable by current experimental techniques. Using MD simulations, poly(3-hexylthiophene) (P3HT) was studied in multiple solvents to probe the effect of solvation on structural properties. Additionally, poly(3-alkylthiophenes) (P3ATs) with side chains varying from two to twelve carbons in length were studied to determine the effect side chain length on these same properties. P3HT was found to have more flexibility in chlorinated solvents, chloroform and dichlorobenzene, than in the other solvents studied. Analysis of the pairwise distribution functions suggests these differences may arise due to the differences in the polymer-solvent interactions. In the case of varying side chain lengths, a counterintuitive inverse proportionality relationship was found between persistence lengths and conjugation lengths. A variety of analyses were unable to illuminate the underlying reason for this inverse relationship.

TABLE OF CONTENTS

1 Introduction and Background 1

2 Methods and Simulation Setup 2
- 2.1 Force Field 2
- 2.2 Simulation Box Setup 5
- 2.3 Persistence Length Calculations 6
- 2.4 Conjugation Length Analysis 7
- 2.5 Pairwise Distribution Functions 8

3 Poly(3-hexylthiophene) in Dilute Solutions 8
- 3.1 Simulation Parameters 8
- 3.2 Structural Properties 9
- 3.3 Torsional Angle Distributions 10
- 3.4 Pairwise Distribution Functions 12
- 3.5 Side Chain End-to-End Distance Distributions 17
- 3.6 Conclusions 18

4 Poly(3-alkylthiophenes) of Varying Side Chain Length in Benzene 21
- 4.1 Simulation Parameters 21
- 4.2 Structural Properties 21
- 4.3 Pairwise Distribution Functions 26
- 4.4 Conclusions 28

5 Future Work 29

6 References 30

1. INTRODUCTION AND BACKGROUND

Conjugated polymers may hold the key for next-generation electronic devices such as solar cell, organic light emitting diodes (OLEDs), organic field-effect transistors (OFETs) and related technologies. Compared with traditional inorganic materials, polymer-based electronic devices are cheaper and lighter, take advantage of abundantly available carbon-based materials, and may have novel features such as flexibility. Furthermore, conjugated polymers such as poly(3-alkylthiophenes) (P3ATs) show self-assembly capabilities in solution, presenting the opportunity for easier processing.[1] Poly(3-hexylthiophene) (P3HT) is commonly studied because due to its relatively rigid π-conjugated backbone, P3HT shows interesting electronic features, while its hexyl side chains allow it to be soluble in a variety of solvents. A connection has been shown between polymer morphology and the electronic properties of resulting devices.[2] Existing experimental techniques, however, are limited in their ability to accurately discern information about polymer structure at the atomic scale.

Molecular dynamics (MD) simulation is a computational technique that allows us to model a system as a collection of particles, and track the positions of these particles over time through numerical integration of Newton's equations of motion:

$$F = m * a = m * \frac{dv}{dt} \qquad [1]$$

MD relies on a defined force field to outline all the bonded (bonds, angles and dihedrals) and non-bonded (Lennard-Jones, electrostatic) interactions in the system. MD simulation generates a trajectory from which measurable quantities

may be calculated, quantities which may be directly comparable to experimental results. There are a few key limitations to MD simulations. One of these limitations is that a simulation will only be as good as the force field used. Classical force fields, for example, are limited in that they do not take into consideration electronic structures. Furthermore, computation time restricts the time and length scales reasonably attainable. However, when all-atom simulations of explicitly solvated polymers are performed, it is possible to provide atomic-level insight into polymer structure that is unavailable by current experimental methods.

2. METHODS AND SIMULATION SETUP

2.1 Force Field

The force field used is modified from the OPLS force field, which is a classical force field with a functional form as follows[3]:

$$E = E_{bonds} + E_{angles} + E_{dihedrals} + E_{nonbonded} \qquad [2]$$

where the potential is a sum of the various bonded and nonbonded interactions present in the system.

The force field parameters used for the P3HT chain were taken from the model proposed and validated by Huang, et al.[4,5] One piece of this model, crucial to accurately capturing polymer folding and unfolding behavior, is the dihedral potential for the angle between adjacent monomers. The model used provides the following cosine series torsional potential:

$$V_{dihed}(\phi) = \sum_{i=0}^{8} c_i * \cos^i(x) \qquad [3]$$

In this equation, c_0 through c_8 are 5.5121, -0.0201, -6.6011, 1.1645, 1.7991, -5.1590, 0.1496, 4.1068, and -0.7607 kcal/mol respectively. In order for this to be compatible with the OPLS force field for use with Gromacs, it needed to fit the Ryckaert-Belleman dihedral form:

$$V_{dihed}(\phi) = \sum_{i=0}^{5} c_i * \cos^i(\psi) \quad [4]$$

$$\phi = \psi - 180° \quad [5]$$

Least squares regression allowed the given model to be fit to the form needed for use in Gromacs. This found constant values for c_0 through c_5 as 29.90598, -1.81205, -25.16036, 10.25222, 2.86207, and -8.57423 respectively. This fitted potential has good fit with the original.

In addition to providing the S-C-C-S dihedral potential, Huang et al. also provide nonbonded (Lennard-Jones) parameters, charges, harmonic bond length parameters, and harmonic bond angle parameters[5]. In order to use these parameters, the oplsaa force field files must be modified. Polymer residues define atom connectivity and charges of those atoms in the file aminoacids.rtp. Each atom in a residue needs a unique name; this is illustrated for a P3HT monomer in Figure 2.1.1. Three unique residues define each polymer: one residue has the C1 atom capped by hydrogen (defining the beginning of a polymer), one residue has the C4 atom capped by hydrogen (defining the end of a polymer) and the third residue caps neither of these atoms allowing it to connect to other monomers on both sides (defining the middle, and most of the monomers in the polymer). Next, bond types, angle types and dihedral types need to be defined in the file ffbonded.itp. The bond types are defined by harmonic bond length potentials, the angle types are defined by

harmonic bond angle potential, and the dihedral types are defined by a dihedral potential in the Ryckaert-Bellemans form. Huang et al. provide all the needed parameters for the thiophene ring; parameters for the alkyl side chain may be borrowed from the OPLS force field values for a hydrocarbon chain. Dihedral angles without given potentials were defined by zeros.

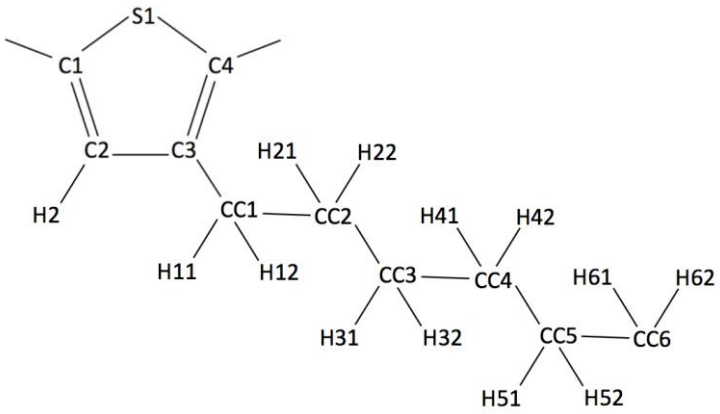

Figure 2.1.1. Atom names for a single P3HT monomer

Solvents benzene, toluene, chloroform, 1,2-dichlorobenzene, and cyclohexane were modeled using the OPLS-AA force field, which has been shown to accurately predict behavior in liquid simulations.[3] Topologies for chloroform and toluene are readily available in literature.[6,7] Topologies for the remaining solvents were defined following the same methods. To verify that the force field accurately solvent chemistry, 10 ns simulations of 1000 solvent molecules in a cubic simulation box were conducted. From these trajectories, density and heat capacity were calculated and compared with experimental values. The first five percent of data points were skipped to ensure averages were representative of equilibrated solvent, and the calculations were performed using three unique simulations to provide information about the error. The results, which can be seen in Table 2.2.1, show

that density can be predicted much more accurately than heat capacity for these five solvents. The heat capacities predicted by simulations show more variation from experiment; this, however, is consistent with similar calculations from literature.[8]

Table 2.2.1. Simulated and experimental solvent densities and heat capacities

	Density [kg/m^3]		*Heat Capacity [J/mol-K]*	
Solvent	*Exp*	*OPLS*	*Exp*	*OPLS*
Benzene	877	867.2 ± 0.4	136	262 ± 3
Toluene	872	845.4 ± 0.1	157	323 ± 1
Chloroform	1479	1396.4 ± 0.4	117	107 ± 1
Dichlorobenzene	1300	1235.9 ± 0.2	114	229 ± 1
Cyclohexane	779	748.2 ± 0.3	156	60 ± 1

2.2 Simulation Box Setup

Packmol was used to generate initial solvation structures for simulation.[8] A single regioregular 60-monomer P3HT chain was positioned with the center of mass at the center of the 15 nm cubic simulation box. An arbitrarily folded conformation of the polymer was used as the starting structure. Solvents chosen include benzene, chloroform, dichlorobenzene and toluene, all of which are solvents typically used with P3HT. Additionally, a poor solvent, cyclohexane, was studied for contrast. The number of solvent molecules in each simulation was selected to approximate the experimental bulk density of the solvent. The systems corresponding to the solvents benzene, toluene, chloroform and o-dichlorobenzene, and cyclohexane contain 222,302, 307,502, 103,502, 205,502, and 325,502 atoms respectively. In order to confirm that the box length was sufficient to allow for rotation and unfolding of the polymer, the maximum polymer dimensions in the x, y and z direction were calculated from the trajectory and compared with the box length. The polymer exceeded the dimensions of the box for only about 5% or less of the simulation

trajectories. Thus, the polymer can rotate and unfold with only minimal self-interaction through the periodic boundary at highly extended, entropically unfavorable states.

2.3 Persistence Length Calculations

Persistence length is a measure of the length of a polymer chain over which fluctuations do not exceed thermal fluctuations and the polymer acts as a rigid rod. It is a measure of the flexibility of a polymer where smaller values relate to a more flexible polymer and larger values relate to a stiffer polymer. The following equation can be used to calculated persistence length (L_p):

$$\langle \cos(\theta(L_c)) \rangle = \exp\left(-\frac{L_c}{L_p}\right) \qquad [6]$$

where L_c is the contour length and $\theta(L_c)$ is the angle between the tangent vector at L_c and the tangent vector at a reference point on the polymer chain. In order to use this equation, snapshots of the polymer backbone from the MD simulations were coarse-grained into a linear polymer by averaging the coordinates of the sulfur atoms from monomers i-1, i and i+1 so that the contribution of each to the average were respectively ¼, ½ and ¼. This coarse-graining is illustrated by Figure 2.3.1. This procedure for calculating persistence length is functionally identical to previous work studying the mechanical properties of actin filaments from AA-MD simulations.[9,10] Since the P3HT polymer chains were longer than the number of monomers needed for a single calculation, the persistence length was averaged from calculations starting from six equally spaced points along the polymer backbone spaced such that each calculation was independent.

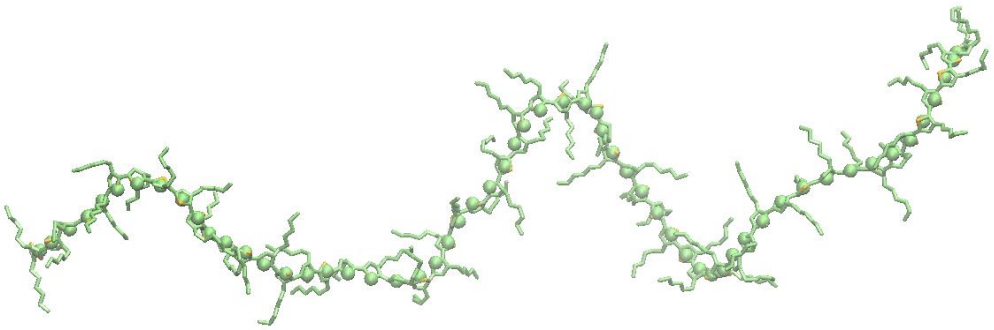

Figure 2.3.1 A coarse-grained P3HT chain (spheres) superimposed onto the corresponding full structure of the polymer. Hydrogen atoms are removed for clarity in the full structure.

2.4 Conjugation Length Analysis

The length along a polymer backbone over which electrons delocalize is the conjugation length. Conjugation lengths provide valuable insight for the design of electronic devices from polymers because it relates directly to electronic properties and device performance. MD simulations do not have the resolution to predict electron positions; therefore, conjugation length cannot be directly calculated. However, from MD simulations it is possible to qualitatively estimate conjugation from the planarity of the torsional angles between adjacent monomers. Brédas and Street used quantum calculations to determine that torsional angles up to 40° away from the planar conformation show only minimal changes in the electronic properties.[11] By assuming that conjugation is not broken for angles within 40° of either 0° or 180° (the cis- and trans- planar conformations respectively), it is possible to determine which torsional angles would break the conjugation. Conjugation length can be approximated using this assumption in two ways: (1) it will be proportional to $1/f$, or the inverse of f, the fraction of conjugation-breaking torsional angles and (2) it will be proportional to the ensemble average of the

maximum number of consecutive planar torsional angles along the polymer backbone.[12,13] The first of these methods will be labeled as 1/f and the second as l_c.

2.5 Pairwise Distribution Functions

The pairwise distribution function, also known as the radial distribution function, provides information about solvent layering around the polymer. It is essentially a histogram of the pairwise distances between atoms or molecules in a system. These were calculated from 5 ns NVT simulations started from the final conformation of the production run trajectories using the GROMACS tool g_rdf. For the simulations of P3HT in various solvents, the pairwise distributions were calculated between specific atoms in the polymer chain and specific atoms in the solvent molecules. For the simulations of P3ATs of varying side chain length, the pairwise distributions were calculated between the center of mass of the backbone atoms for each monomer and the center of mass of the benzene molecules. Bin widths of 0.008 nm or 0.012 nm were used as needed to smooth the curves.

3. POLY(3-HEXYLTHIOPHENE) IN DILUTE SOLUTIONS

3.1 Simulation Parameters

MD simulations were performed using the GROMACS 4.5.5 package.[14] Each system was subject to steepest decent energy minimization until the maximum force reached a tolerance of 10 kJ mol^{-1} nm^{-1}. The minimized system was simulated for 1 ns in the NVT ensemble in order to allow the bonds to relax. The next 4 ns of NPT

simulation allowed the box dimensions to adjust to equilibrate the density of the solvent. Following this, production runs of length 150 ns were performed in the NVT ensemble. Two repeat simulations were completed for each solvent. Temperature was held constant in all simulations at 300 K using a stochastic global thermostat.[15] Simulations in the NPT ensemble used the Berendsen barostat.[16] All MD simulations used a time step of 2 fs and LINCS constraints on all bonds.[17] Pairwise distribution functions were calculated using the g_rdf tool from GROMACS from an additional 5 ns of NVT simulation started from the end of each production run. This was done for both repeat simulations for each solvent, and the difference between repeat simulations was negligible.

3.2 Structural Properties

Persistence length and conjugation length calculations are shown in Table 3.2.1. Persistence lengths for the non-chlorinated solvents, benzene, toluene and cyclohexane, were similar and greater than those of the chlorinated solvents, chloroform and dichlorobenzene. The conjugation lengths follow a similar, consistent trend. It is important to note that these conjugation lengths provide qualitative information proportional to conjugation length rather than being an exact calculation.

Table 3.2.1. Structural quantities for P3HT in five different solvents.

Solvent	l_p *[nm]*	*1/f [nm]*	l_c *[nm]*
Benzene	3.36 ± 0.17	7.61 ± 0.02	12.69 ± 0.01
Toluene	3.36 ± 0.19	6.70 ± 0.03	11.95 ± 0.05
Chloroform	3.22 ± 0.04	5.42 ± 0.04	10.71 ± 0.03
Dichlorobenzene	3.03 ± 0.02	5.02 ± 0.02	10.27 ± 0.02
Cyclohexane	3.35 ± 0.04	7.73 ± 0.03	12.75 ± 0.004

3.3 Torsional Angle Distributions

Two planar conformations are possible for the intermonomer dihedral angle of P3HT: the cis-conformation occurs when this angle is 0° and the trans-conformation at 180°. As shown by Figure 3.3.1, most of the intermonomer dihedral angles fall within about 40° of one of these two planar conformation. The trans-conformation is preferred, likely because this is the conformation which minimizes the intereactions between side chains of adjacent monomers. This potential may also be used to calculate a free energy plot, shown in Figure 3.3.2, from the following equation:

$$\Delta G = -kTln\left(\frac{P}{P_{max}}\right) \qquad [7]$$

where ΔG is the free energy, k is the Boltzmann constant, T is the temperature, and P is the probability. The result provides information about the energy barrier which must be overcome in order for a monomer to rotate relative to an adjacent monomer. This energy barrier to rotation is consistent with the structural properties shown in the previous section; in the solvents where P3HT is more flexible as calculated by the persistence lengths, chloroform and dichlorobenzene, the free energy barrier to rotation is is lower.

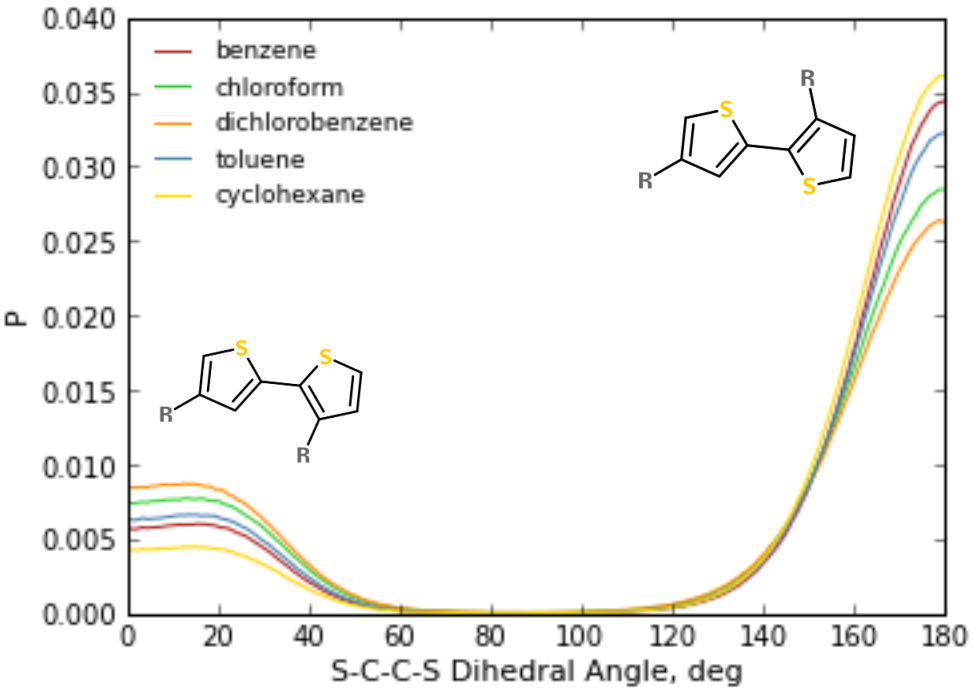

Figure 3.3.1. Histogram of the distribution of the dihedral angle between adjacent monomers for P3HT in five solvents is shown with inset images illustrating the two planar conformations.

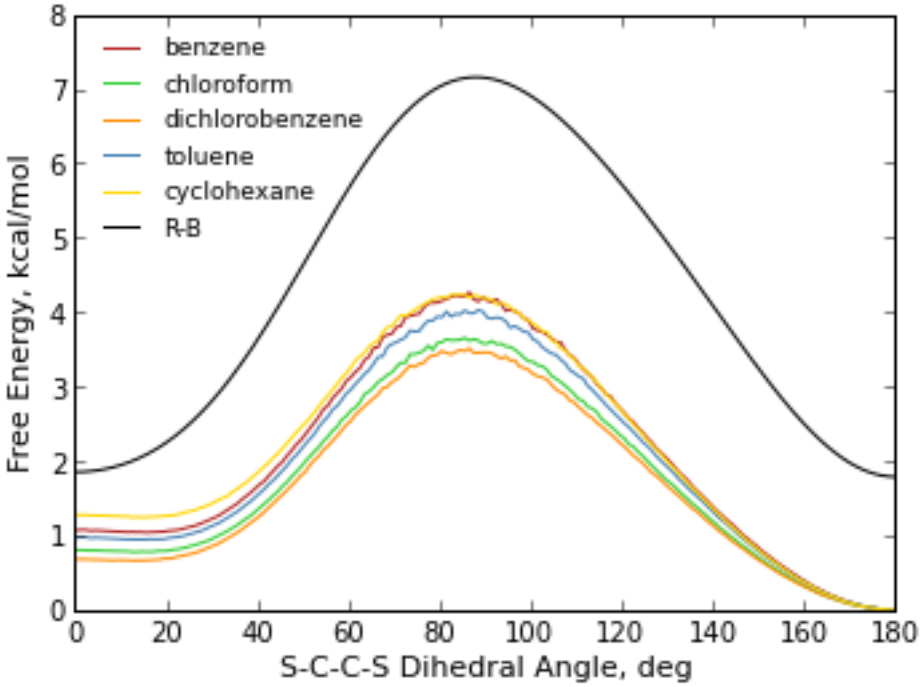

Figure 3.3.2. Free energy plot for the dihedral angle between adjacent monomers for P3HT in five solvents is shown along with the Ryckaert-Bellmans potential corresponding to this dihedral as modeled by the applied force field.

3.4 Pairwise Distribution Functions

In this analysis, pairwise distributions, g(r), were calculated between specific atoms on the polymer and solvent structures. Since solvents of different sizes and shapes were used, it is impossible to draw a direct comparison between pairwise distributions if the centers of mass are used. Figure 3.4.1 shows the pairwise distributions between the various atoms in the polymer backbone while averaging out the various solvent atoms. In all five solvents, g(r) is less than one in the vicinity of the polymer backbone. A value of one for g(r) means that the density at that radius is equivalent to the bulk density. This lower value likely results largely from the exclusion of solvent molecules from the volume occupied by the polymer chain. Also, all solvent molecules pack more closely around the sulfur and C2 carbon atoms than the other atoms in the thiophene ring. This is likely explained because the other atoms in the backbone are connected to either other monomers (C1 and C4) or the hexyl side chain (C3) and steric hindrance would prevent solvent molecules from closely packing around these atoms.

It is also possible to perform these pairwise distribution function calculations by decomposing the solvent molecules into specific sites. When this is done, atoms that are equivalent by symmetry do not provide unique curves. For example, in the toluene atom, illustrated in Figure 3.4.2, atoms C2 and C6 are equivalent as are atoms C3 and C5. Keeping in mind the symmetry, carbon atoms in toluene can be decomposed into five unique curves, and the carbon and chlorine atoms in dichlorobenzene can be decomposed into four unique curves.

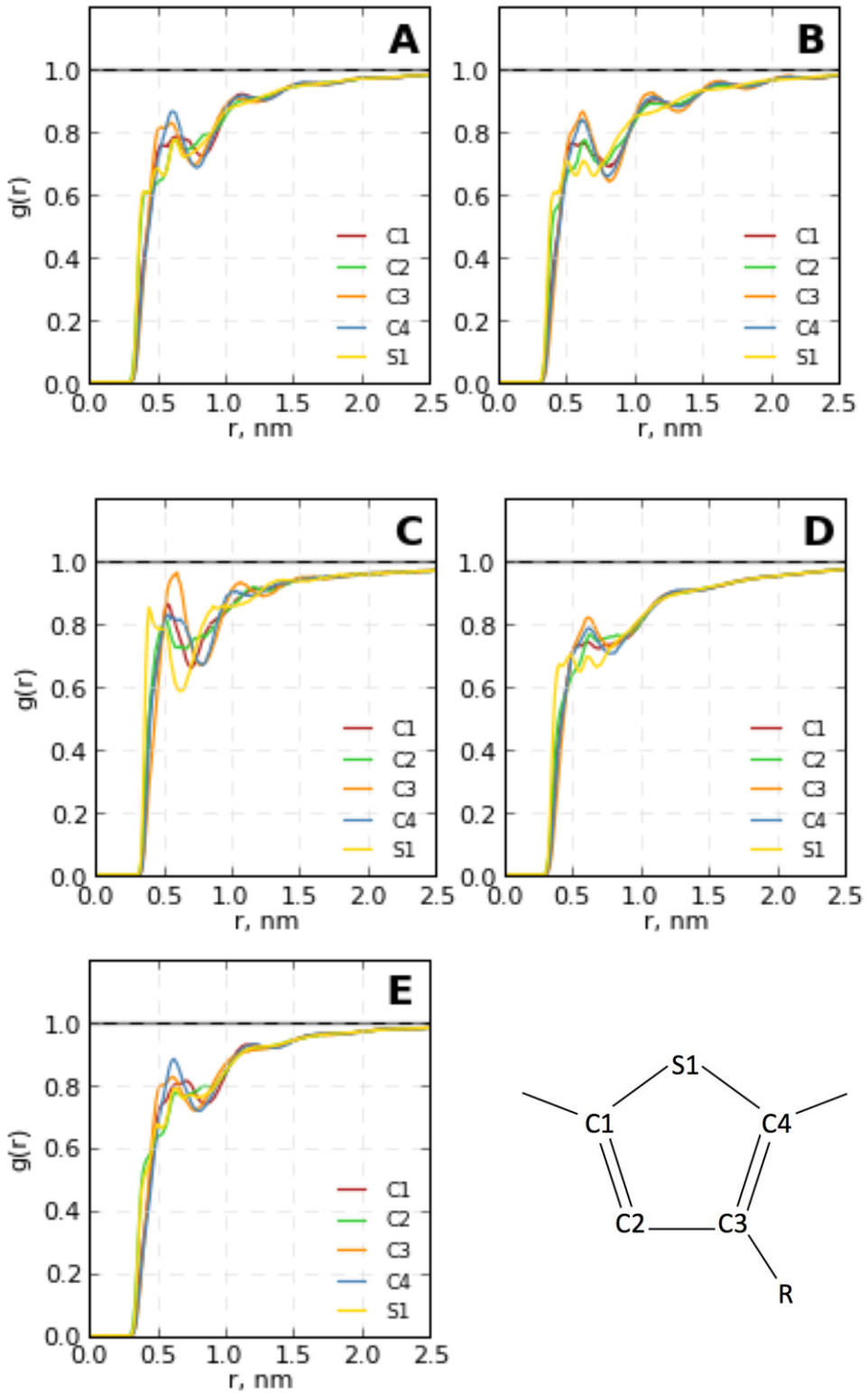

Figure 3.4.1. Pairwise distribution functions relating specific sites along the P3HT backbone to the carbon atoms in the five solvent molecules: (A) benzene, (B) cyclohexane, (C) chloroform, (D) dichlorobenzene, (E) toluene. Specific backbone sites have are decomposed into different curves, wheras sites in the solvent molecules have are averaged out.

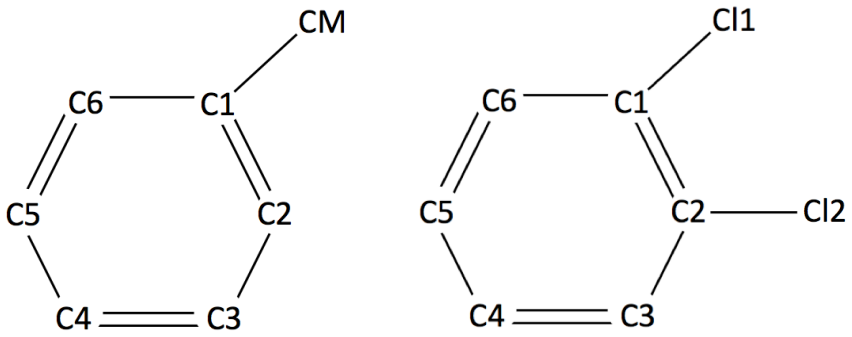

Figure 3.4.2. Chemical structures for toluene (left) and dichlorobenzene (right) illustrating atom naming.

Figure 3.4.3 shows the pairwise distribution functions between two specific atoms on the P3HT backbone and the specific atoms on the toluene molecules, and Figure 3.4.4 shows these for dichlorobenzene molecules. These two figures illustrate that there is a preferential orientation of the solvent molecules around the polymer chain. In toluene, the solvent molecules are more likely to orient such that the methyl group is closer to the polymer chain than the aromatic ring. In contrast, dichlorobenzene is more likely to orient with the chlorine atoms further from the polymer chain than the aromatic ring. These differences in solvent packing may be responsible for the variations in structural properties of P3HT in various solvents.

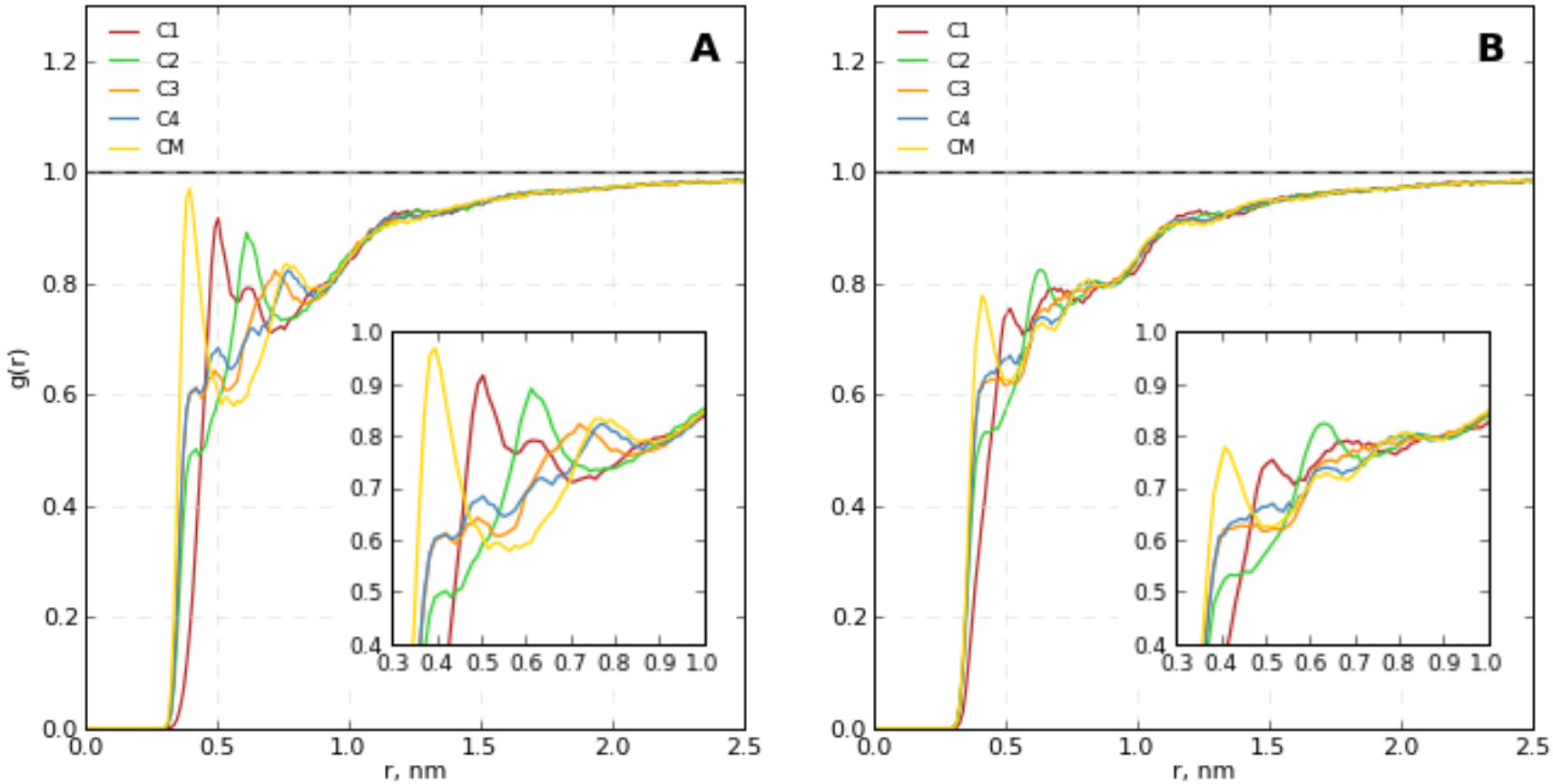

Figure 3.4.3. Pairwise distribution functions relating the one specific atom in the polymer backbone, (A) sulfur or (B) C2, to specific atoms in the toluene solvent molecules. Specific solvent sites have been decomposed into different curves, and the insets zoom in on the first set of peaks.

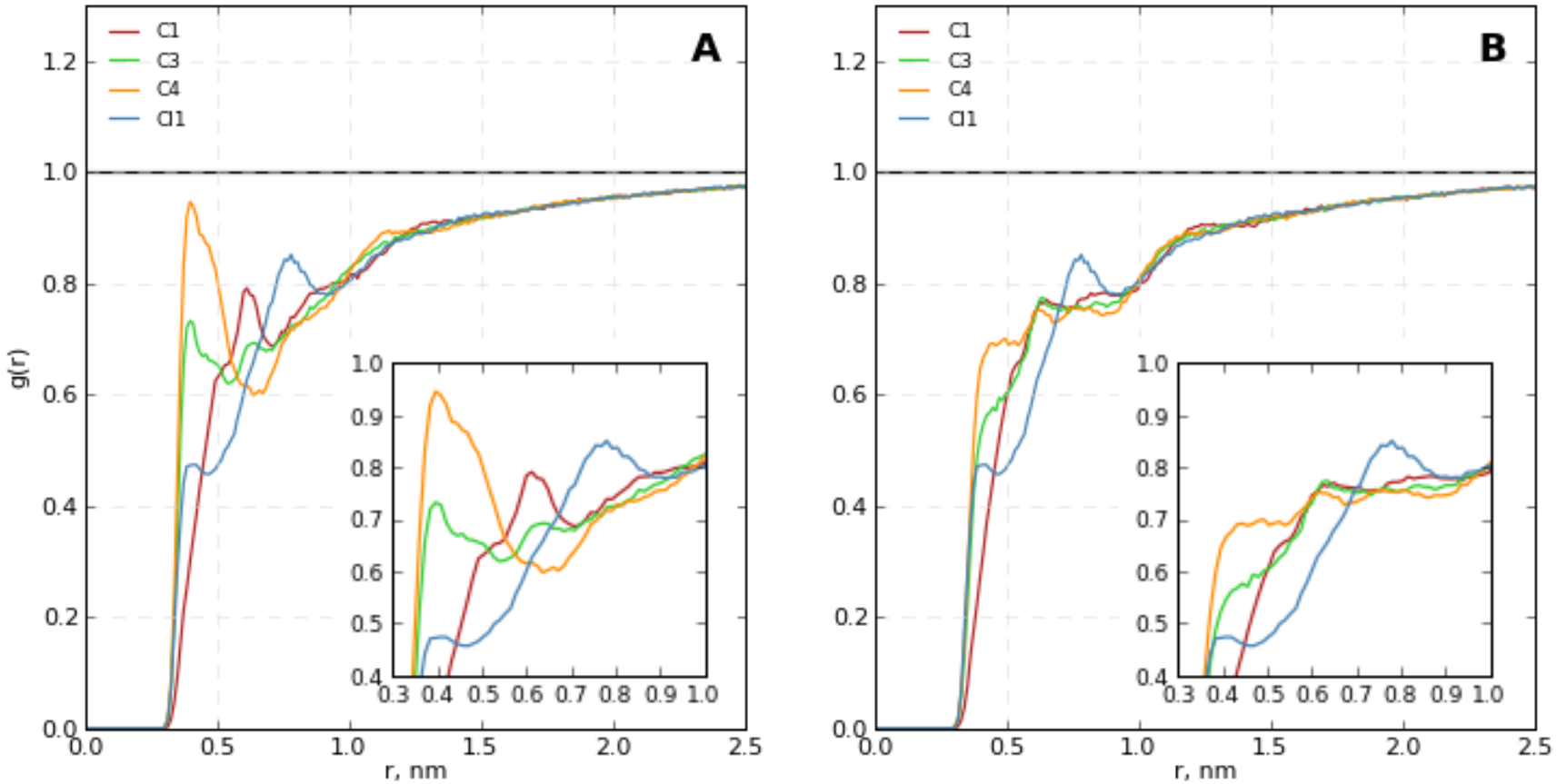

Figure 3.4.4. Pairwise distribution functions relating the one specific atom in the polymer backbone, (A) sulfur or (B) C2, to specific atoms in the dichlorobenzene solvent molecules. Specific solvent sites have been decomposed into different curves, and the insets zoom in on the first set of peaks.

3.5 Side Chain End-to-End Distance Distributions

Side chain conformational differences in the various solvents were explored as one possible explanation for the in chain flexibilities. Figure 3.5.1 shows the distribution of end-to-end distances for the P3HT hexyl side chains. The three visible peaks at 6.0, 7.0 and 7.6 Å correspond to hexyl side chains with two cis-torsional angles, one cis-torsional angle, and all trans-torsional angles respectively. The hexyl side chain of P3HT is more likely to be fully extended in benzene or toluene than in chlorinated solvents. It is possible arise due to differences in interactions between the side chain and nearby solvent molecules.

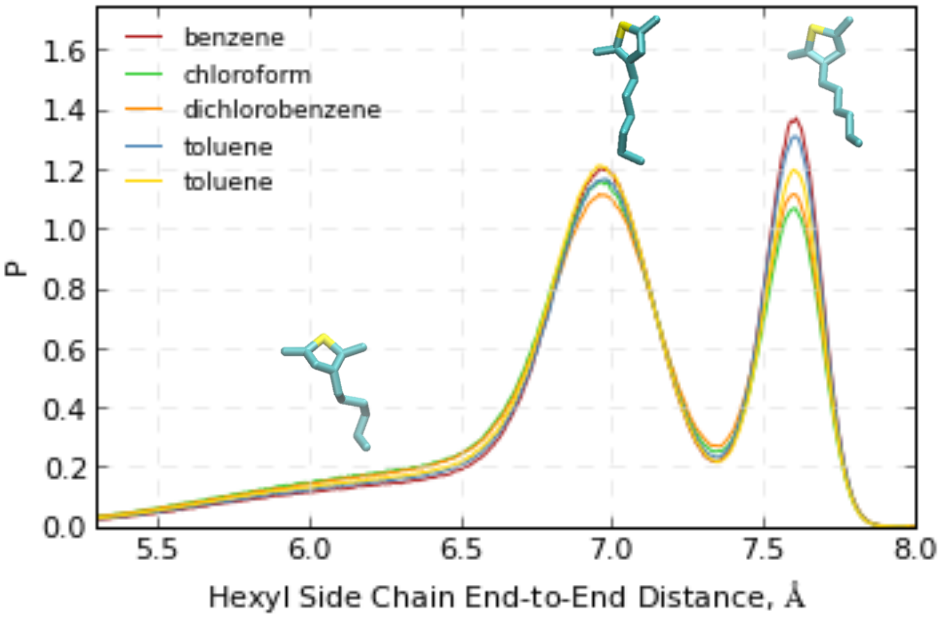

Figure 3.5.1. Histogram of the end-to-end distances of the P3HT hexyl side chain in solvents using a bin width of 0.009 Å. A sample side chain conformations is shown above each peak.

To further explore the relationship, hexane chains were simulated in solvent. 250 hexane chains and 300 solvent molecules were placed at random inside a 5 nm simulation box. A histogram of the end-to-end distances for the hexane chains was

constructed from 20 ns of NVT simulation. As shown in Figure 3.5.2, there was no appreciable difference in hexane folding when solvated with benzene, chloroform, dichlorobenzene or toluene. Also notable is that a much higher proportion of the chains were fully extended than in the case of the hexyl side chains. It would appear that being attached to the P3HT backbone, and the confinement resulting from that, is significant for the differences seen in Figure 3.5.1.

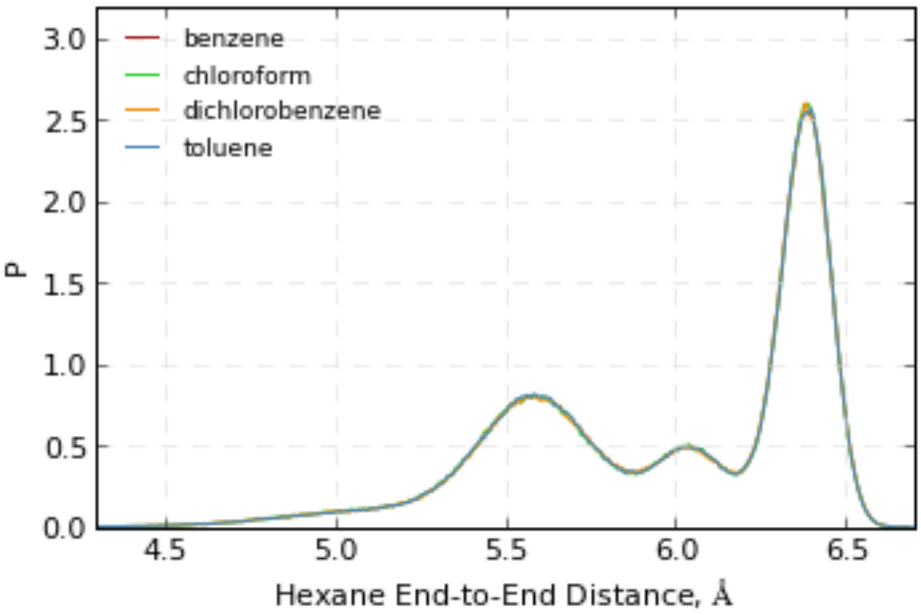

Figure 3.5.2. Histogram of the end-to-end distances of hexane chains in solvents.

3.6 Conclusions

Solvent plays a role in determining the structural properties of a P3HT chain in dilute solution. MD simulations have consistently shown that in chloroform or dichlorobenzene, P3HT is more flexible, and has a lower conjugation length than in the other three solvents studied. This difference is consistent with the free energy barrier for rotation of the intermonomer torsional angle. Pairwise distribution

functions can help to illuminate possible explanations for why these differences arise by allowing a more detailed look at interactions between solvent and polymer. For example, these simulations have shown that solvents have a preferential orientation around the polymer chain. In chlorinated solvents, chlorine atoms are preferentially shielded from the polymer by the rest of the solvent atom. In contrast, toluene atoms preferentially pack around the polymer with the methyl group pointed towards the polymer. Furthermore, it has been shown that it is possible that interactions between solvent and side chains cause differences in polymer properties.

Cyclohexane was chosen for simulation because it is a poor solvent for P3HT. This means the polymer would be expected to coil up and interact preferably with itself over nearby solvent molecules. With this in mind, it might be expected that simulation would yield dramatically different results for P3HT solvated in benzene when compared to P3HT solvated in cyclohexane. However, this was not the case. Looking closer at the applied force field helps to explain why this is not a surprising result. Figure 3.6.1 illustrates the Lennard-Jones potentials used for the non-bonded interactions between carbon and other atoms. In comparison, Figure 3.6.2 illustrates that there are only minimal differences between the potentials used for sp^2 and sp^3 carbons in the model used. The force field does not take into consideration electronic effects, such as π-stacking, which might differentiate between otherwise very similar cyclohexane and benzene molecules.

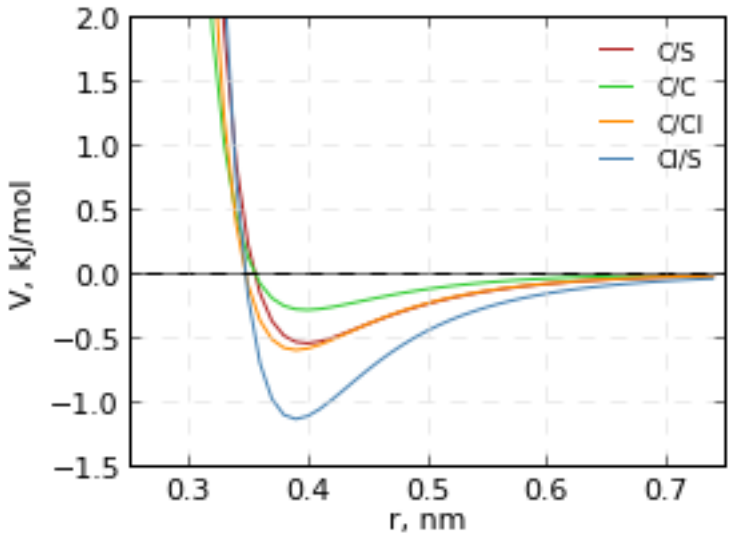

Figure 3.6.1 Lennard-Jones potentials for the interactions between atom types used in simulations of P3HT in solutions.

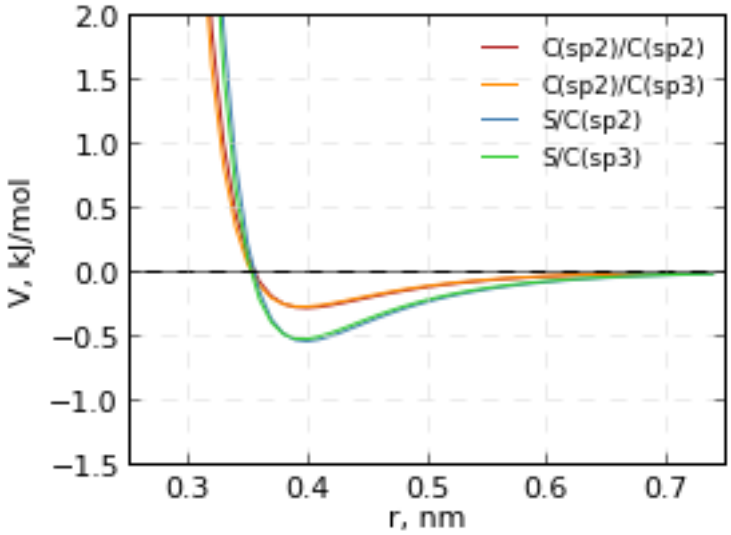

Figure 3.6.2 Lennard-Jones potentials for the interactions between atom types used in simulations of P3HT in solutions.

4. POLY(3-ALKYLTHIOPHENES) OF VARYING SIDE CHAIN LENGTH IN BENZENE

4.1 Simulation Parameters

Most methods used for MD simulations of P3ATs of differing side chain length were identical to those used for simulations of P3HT in various solvents as described in Section 3.1. Only the differences in the methods will be described here. Polymers used are regioregular 60-monomer chains of poly(3-ethylthiophene) (P32T), poly(3-butylthiophene) (P34T), poly(3-hexylthiophene) (P3HT), poly(3-octylthiophene) (P3OT), and poly(3-dodecylthiophene) (P3DDT) in benzene. These polymers are P3ATs with linear alkyl side chains of 2, 4, 6, 8, and 12 carbons length. In order to accommodate the extra volume of the 12-carbon side chains, simulations of P3DDT used a 16 nm simulation box. P34T and P3OT were simulated using GROMACS 4.6.5 in order to take advantage of the increased speed as compared to previous versions of GROMACS. Repeat simulations were not performed.

4.2 Structural Properties

Stiffer polymers might be expected to have higher conjugation length, however, experimental findings have shown that this is not necessarily the case. Figure 4.2.1, shows a loose trend towards decreasing absorption peak as Kuhn length increases. In looking at this figure, note that Kuhn length is a measure of flexibility equal to twice the persistence length, and that red-shifted absorption profiles are expected for polymers with higher conjugation lengths. MD simulations provide the opportunity to look at the polymer properties and structures on the atomic scale in order to further understand this relationship.

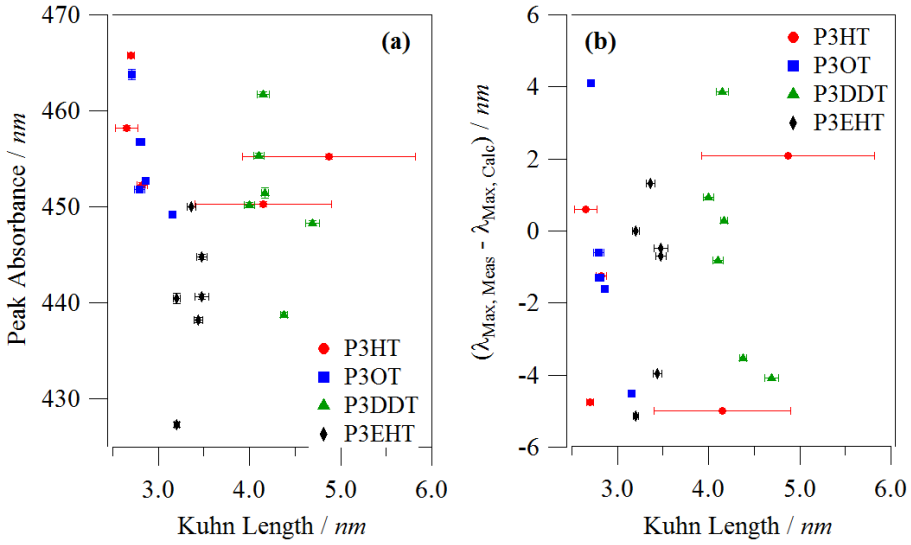

Figure 4.2.1. (a) peak absorbance, from UV-vis, plotted against Kuhn length for P3ATs in benzene, toluene, chloroform, o-dichlorobenzene, chlorobenzene, and cyclohexane. (b) Difference between calculated peak absorbance and measured peak absorbance plotted against Kuhn length (unpublished experimental data from Gregory Newbloom)

Using simulations, it was possible to confirm that P3ATs were generally found to have higher persistence lengths and lower conjugation lengths with increasing side chain length. This is illustrated by simulation results in Figure 4.2.2. This inverse relationship is more clearly demonstrated when these two quantities are plotted against each other in Figure 4.2.3. However, the same inverse relationship was not seen in the previous study of P3HT in various solvents. The remainder of the analyses presented here provides an attempt to determine a mechanism for this relationship.

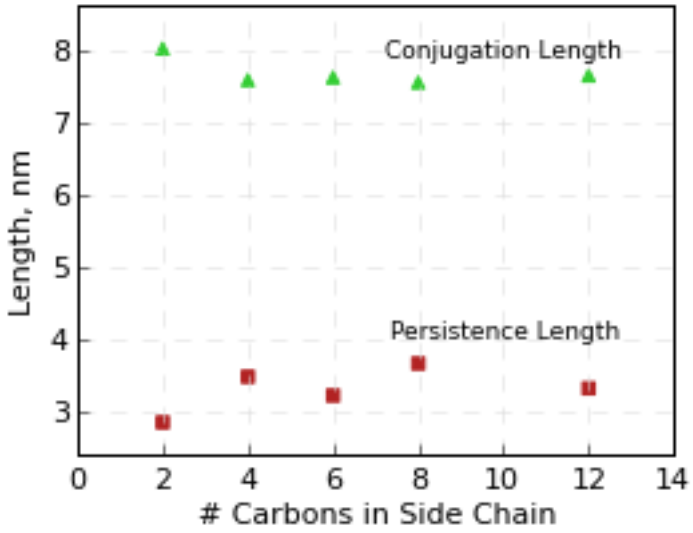

Figure 4.2.2. Conjugation length and persistence length plotted against side chain length for P3ATs.

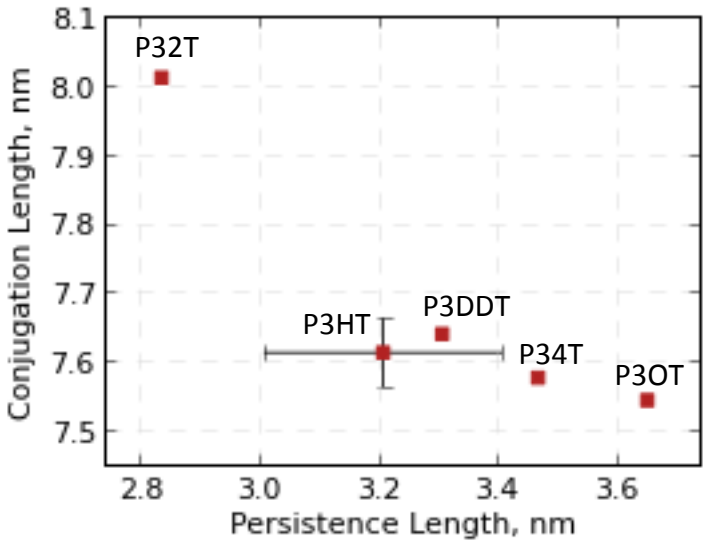

Figure 4.2.3. Conjugation length plotted against persistence length for P3ATs of different side chain length.

The minimum radius of gyration is larger for polymers with longer side chains, but the maximum radius of gyration is fairly similar among all studied polymers as shown in Figure 4.2.4. This result is expected because without the bulk of the longer sides, P3AT is able to fold much more tightly than the other polymers. Simulation snapshots clearly illustrate these differences in Figure 4.2.5 as there is a much more significant difference between the structures at the minimum radius of gyration than at the maximum. This can explain the trend toward smaller persistence lengths for polymers with longer side chains since a polymer that can fold more tightly may reasonably be assumed to be less rigid.

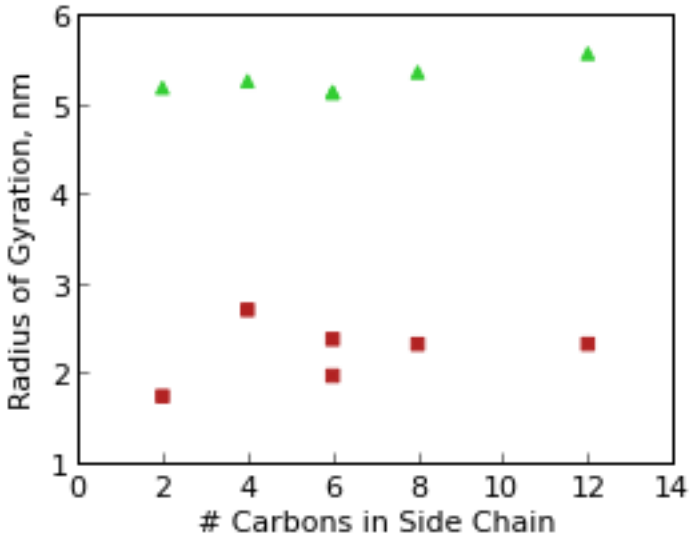

Figure 4.2.4. Minimum (squares) and maximum (triangles) radius of gyration plotted gainst side chain length for five P3ATs.

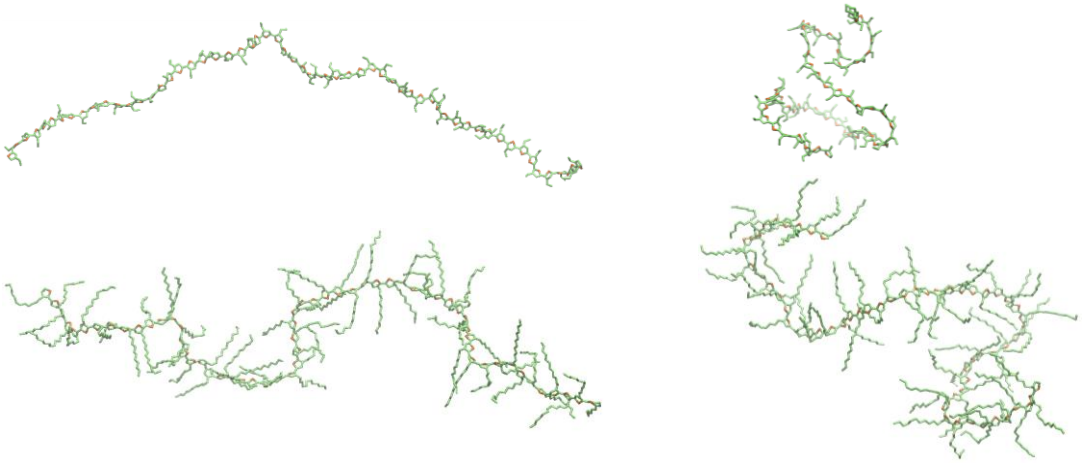

Figure 4.2.5. Conformational differences btween the maximum (left) and minimum (minimum) radius of gyration observed radius of gyration are illustrated for P32T (top) and P3DDT (bottom). Hydrogen atoms have been removed for clarity.

Conjugation length was calculated separately for folded and extended polymer segments to test the hypothesis that folds in a polymer stabilize the planar dihedral angles in order for conjugation length to be higher for more flexible polymers. Each polymer was broken into segments 11 monomers in lengths. The end-to-end distance of each segment was compared to the average end-to-end distance for segments of that length. If the end-to-end distance of the segment was more than one standard deviation above the average it was considered to be extended, and if the end-to-end distance was more than one standard deviation lower than the average it was considered folded. This is illustrated by Figure 4.2.6. Conjugation length was calculated for these types of segments separately by the 1/f method and these results are outlined for all five P3ATs in Table 4.2.7. There doesn't seem to be a pattern to whether folded or unfolded segments have higher conjugation length.

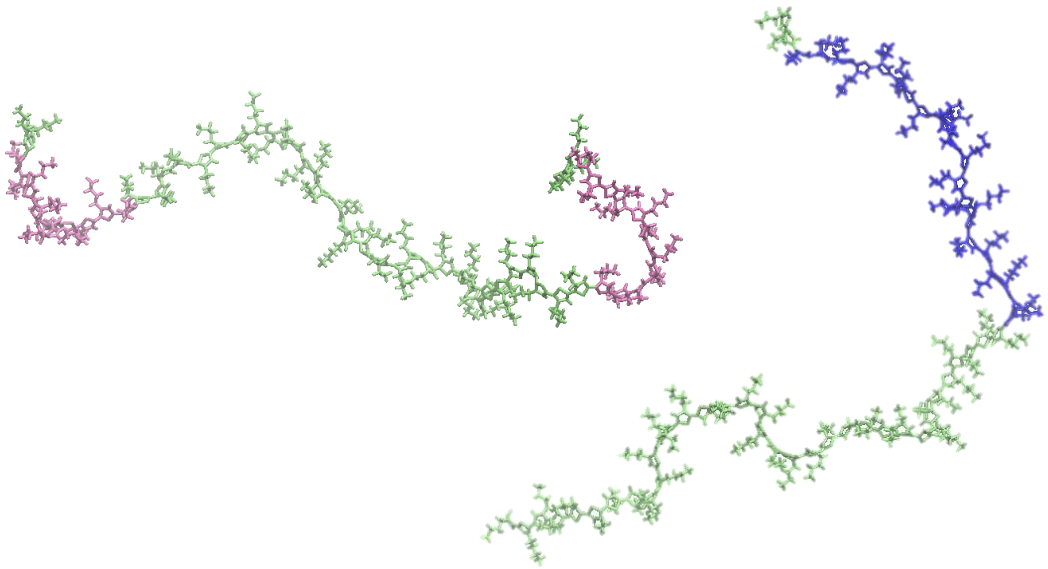

Figure 4.2.6. Two P34T conformations with folded segments highlighted in pink and an extended segment highlighted in blue.

Table 4.2.7 Conjugation lengths calculated from the full polymer as well as folded and extended 11-monomer segments

	P32T	P34T	P3HT	P3OT	P3DDT
Full L_c [nm]	8.01	7.57	7.61	7.54	7.39
Folded L_c [nm]	8.34	7.39	8.04	7.39	7.30
Extended L_c [nm]	7.91	7.64	7.75	7.70	7.56

4.3 Pairwise Distribution Functions

Pairwise distribution functions were calculated relating the center of mass of the backbone atoms to the center of mass of the benzene rings in order to compare the solvent layering around the polymers of caused by varying side chain lengths. These are shown in Figure 4.3.1. The peak heights of the first two peaks roughly inversely follow the order of side chain length, that is, the peak heights are largest for P3ATs with the shortest side chains. This would suggest that the bulk of the longer side chains may affect the ability of solvent molecules to pack in the near vicinity of the chain.

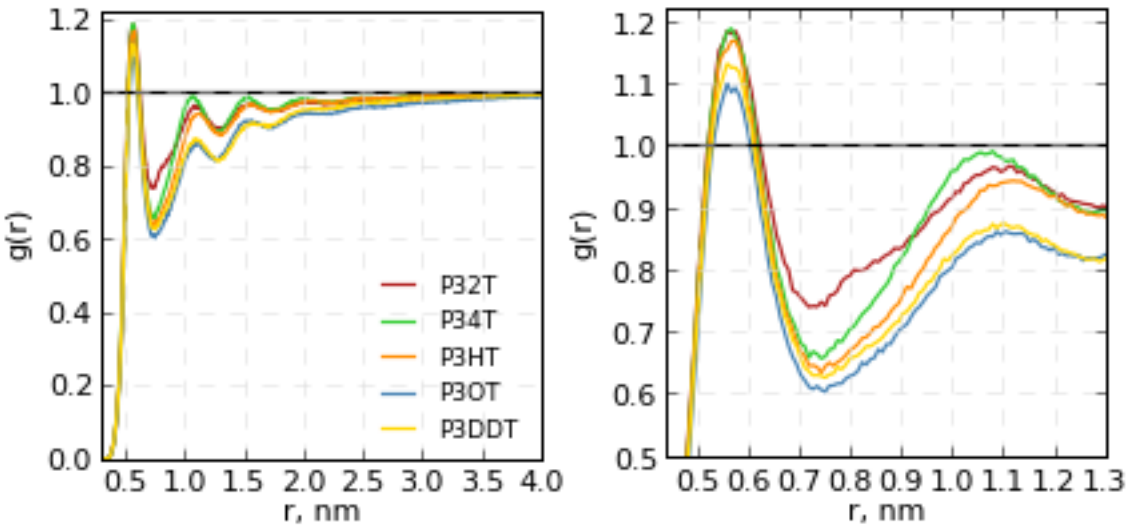

Figure 4.3.1. Pairwise distribution functions relating the center of mass of the P3AT backbone atoms to the center of mass of the benzene carbon atoms. The image on the right zooms in on the first two peaks to better illustrate these features.

In order to determine if polymer conformation influences the pairwise distribution, four polymer conformations were selected from simulations of P3OT with a radius of gyration of 26 and four were selected with a radius of gyration of 50. The backbone atoms were frozen during a 5 ns NVT simulation. The resulting pairwise distribution functions were calculated and the results are shown in Figure 4.3.2. All eight pairwise distributions obtained by this method had higher first and second peak than the original distribution with no discernable difference between those calculated from the highly folded structure and those from the extended structure. PLUMED 2 was also used to constrain the radius of gyration of two solvated P3OT chains. An upper wall was used to constrain the radius of gyration of one chain to below 28 Å and a lower wall constrained the radius of gyration of the second chain to above 50 Å. Both chains were simulated in the NVT ensemble for 5 ns then pairwise distributions were calculated from the trajectories. This method

produced similar results to those shown in Figure 4.3.1. The packing of solvent molecules does not seem to be discernably different between folded and unfolded polymer structures.

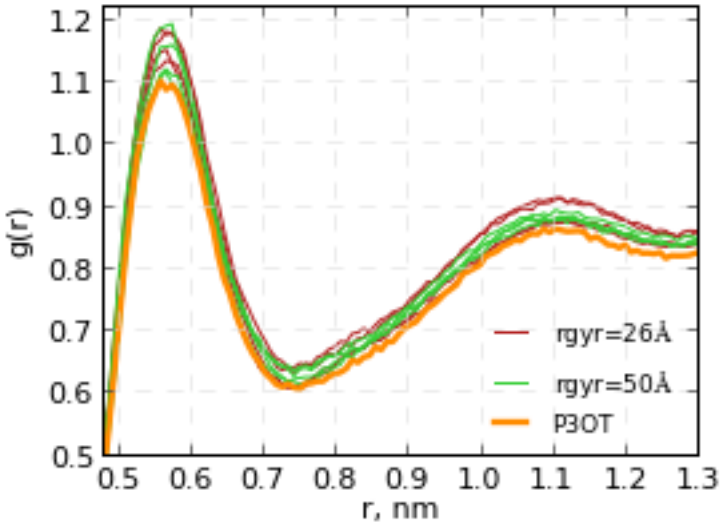

Figure 4.3.2. Pairwise distribution functions relating the center of mass of the P3OT backbone atoms to the center of mass of the benzene carbon atoms. The thick orange line is the originally calcluated distribution and the other lines were calculated from polymers with backbone atoms frozen at a radius of gyration of 26 Å (red) or 50 Å (green).

4.4 Conclusions

When solvated P3ATs of varying side chain lengths are simulated, some of the results were as expected. These results rely on the differences in steric effects between bulky side chains eight or twelve carbons in length and much smaller side chains of two or four carbons in length. Solvent molecules were able to pack more tightly around polymers with shorter side chains. Also, polymers with less bulky side chains were able to fold into much more compact conformations than those with longer side chains. Less intuitive was the result that polymers with longer side chains tend to have higher conjugation lengths, but lower persistence lengths. The

implication of this inverse relationship is that more flexible polymers have few planar segments. A variety of hypotheses as to why this might occur were studied. However, the analyses performed were unsuccessful at determining why conjugation length is inversely related to persistence length.

5. FUTURE WORK

The work presented here shows that although there are some limitations, molecular dynamics simulation can be an interesting tool for exploring conjugated polymers such as P3ATs. One possible future direction would be to study longer polymer chains, which would allow for more direct comparison with experiment and provide opportunity for further exploring the structures that might arise as a result of self-interactions. One challenge in expanding simulations to longer polymer chains is the extra computational time required. Two possible methods to overcome this obstacle would be using a coarse-grained force field to decrease the number of particles in the system, or to employ enhanced sampling techniques such as metadynamics in order to explore the phase space more efficiently. Design of simulations to study chain-chain interactions would also be interesting because of the implications for polymer self-assembly. A better understanding of the interactions involved in self-assembly would provide valuable insight into the design of processing techniques and the creation of electronic devices. Finally, as real polymers are never fully regioregular or without defect, it may be insightful to study the effects of chain defects on both the local and full chain length scales.

6. REFERENCES:

1. Bao, Z., Dodabalapur, A. & Lovinger, A. J. Soluble and processable regioregular poly(3-hexylthiophene) for thin film field-effect transistor applications with high mobility. *Appl. Phys. Lett.* **69,** 4108–4110 (1996).

2. Kline, R. J. *et al.* Dependence of regioregular poly(3-hexylthiophene) film morphology and field-effect mobility on molecular weight. *Macromolecules* **38,** 3312–3319 (2005).

3. Jorgensen, W. L., Maxwell, D. S. & Tirado-rives, J. Development and Testing of the OPLS All-Atom Force Field on Conformational Energetics and Properties of Organic Liquids. **7863,** 11225–11236 (1996).

4. Do, K., Huang, D. M., Faller, R. & Moulé, A. J. A comparative MD study of the local structure of polymer semiconductors P3HT and PBTTT. *Phys. Chem. Chem. Phys.* **12,** 14735–9 (2010).

5. Huang, D. & Faller, R. Coarse-grained computer simulations of polymer/fullerene bulk heterojunctions for organic photovoltaic applications. *J. Chem. Theory …* **6,** 526–537 (2010).

6. Caleman, C. *et al.* Force Field Benchmark of Organic Liquids : Density , Enthalpy of Vaporization , Heat Capacities , Surface Tension , Isothermal Compressibility , Volumetric Expansion Coefficient , and Dielectric Constant. *J. Chem. Theory Comput.* **8,** 61–74 (2012).

7. Van der Spoel, D., van Maaren, P. J. & Caleman, C. GROMACS molecule & liquid database. *Bioinformatics* **28,** 752–3 (2012).

8. Martínez, L., Andrade, R., Birgin, E. G. & Martínez, J. M. Software News and Update Packmol : A Package for Building Initial Configurations for Molecular Dynamics Simulations. *J. Comput. Chem.* **30,** 2157–2164 (2009).

9. Chu, J.-W. & Voth, G. a. Allostery of actin filaments: molecular dynamics simulations and coarse-grained analysis. *Proc. Natl. Acad. Sci. U. S. A.* **102,** 13111–6 (2005).

10. Pfaendtner, J., Lyman, E., Pollard, T. D. & Voth, G. a. Structure and dynamics of the actin filament. *J. Mol. Biol.* **396,** 252–63 (2010).

11. Brédas, J. & Street, G. Organic polymers based on aromatic rings (polyparaphenylene, polypyrrole, polythiophene): Evolution of the electronic properties as a function of the torsion angle. *J. Chem. Phys.* **83,** 1323–1329 (1985).

12. Cells, N. P. H. T. S., Bernardi, M., Giulianini, M. & Grossman, J. C. Self-Assembly and Its Impact on Interfacial Charge Transfer in Carbon. **4,** 6599–6606 (2010).

13. Zhang, G., Pei, Y., Ma, J., Yin, K. & Chen, C.-L. Packing Structures and Packing Effects on Excitation Energies of Amorphous Phase Oligothiophenes. *J. Phys. Chem. B* **108,** 6988–6995 (2004).

14. Pronk, S. *et al.* GROMACS 4.5: a high-throughput and highly parallel open source molecular simulation toolkit. *Bioinformatics* **29,** 845–54 (2013).

15. Bussi, G., Donadio, D. & Parrinello, M. Canonical sampling through velocity rescaling. *J. Chem. Phys.* **126,** 014101 (2007).

16. Berendsen, H. J. C., Postma, J. P. M., van Gunsteren, W. F., DiNola, a. & Haak, J. R. Molecular dynamics with coupling to an external bath. *J. Chem. Phys.* **81,** 3684 (1984).

17. Hess, B. P-LINCS: A Parallel Linear Constraint Solver for Molecular Simulation. *J. Chem. Theory Comput.* **4,** 116–122 (2008).